

13.2

Low-energy ion scattering with additional mass separation: instrumentation and application

© A.B. Tolstoguzov^{1–3}, S.I. Gusev¹, D.J. Fu³

¹ Ryazan State Radio Engineering University, Ryazan, Russia

² Centre for Physics and Technological Research, Universidade Nova de Lisboa, Caparica, Portugal

³ Innovation Center of Tsinghua University Research Institute in Zhuhai, Zhuhai, China

E-mail: a.tolstoguzov@fct.unl.pt

Received June 22, 2022

Revised November 3, 2022

Accepted November 7, 2022

Hardware implementation and application of the combined energy and mass spectrometric analysis of backscattered and sputtered ions are discussed. For a ternary jewelry alloy contained Au, Ag and Cu, it was shown that this method is able improving analytical sensitivity by suppressing the background related to sputtered ions, and with heavy Ar⁺ ions to obtain information on the surface condition of a lanthanum sample and to detect backscattered and sputtered Ar²⁺ ions on this surface.

Keywords: ion scattering, ion sputtering, mass spectrometric analysis, energy spectra, lanthanum

DOI: 10.21883/TPL.2023.01.55344.19286

Low-energy ion scattering (LEIS) [1,2] is an analytical technique that is used to characterize the elemental composition of surfaces and is based on the model of binary elastic collisions between primary ions (in most cases, inert gases) and surface atoms. The classical LEIS version involves energy analysis of ions scattered by angle θ relative to the direction of primary ions. The energy and momentum conservation laws provide an opportunity to determine mass M of surface atoms the collision with which alters the trajectory of motion of (backscattered) primary ions with mass M_0 :

$$M = M_0 \frac{1 + E/E_0 - 2 \cos \theta \sqrt{E/E_0}}{1 - E/E_0}, \quad (1)$$

where $M > M_0$ and E_0 and E are the kinetic energies of a primary ion before and after a collision with a surface atom, respectively.

The energy analysis of scattered ions in LEIS is performed using various types of electrostatic analyzers (usually cylindrical or spherical deflectors). Time-of-flight analyzers with pulse modulation of the primary beam have also been used [3]. In both cases, the energy analysis does not allow one to completely separate sputtered ions, which are also produced in the interaction of primary ions with surface atoms, from backscattered ones. Sputtered ions produce a peak with a near-zero energy in LEIS spectra and are considered as a background that makes it more difficult to determine the elemental composition of the studied sample.

The problem of suppression of the sputtered-ion background was solved in a Qtac [4] setup that is produced by ION-TOF and combines a pulsed source of primary ions with time-of-flight cleaning of analyzed ions, which is implemented in a specialized toroidal electrostatic energy

analyzer [5]. This LEIS modification is referred to as high-sensitivity low-energy ion scattering (HS-LEIS) in literature. HS-LEIS is now being used successfully to study catalysis, adhesion, oxidation, thin-film synthesis, and other surface processes (see, e.g., [6,7] and references therein). Cleaning (i.e., suppression of the contribution of sputtered ions to the energy spectrum) is especially efficient when light ⁴He⁺ ions are used as primary ones. However, the mass-spectral resolution of LEIS (its possibility to resolve peaks of ions backscattered from atoms with close masses) decreases considerably as ratio M/M_0 increases. Therefore, helium ions do not provide reliable results in LEIS/HS-LEIS analysis of the surface of samples containing atoms of several elements with close masses in the range of $M > 70–100$ amu. Heavier primary ions, such as ²⁰Ne⁺ or even ⁴⁰Ar⁺, are needed for this purpose. When these primary ions are used, the intensity of sputtered ions increases accordingly.

A combined mass-spectral and energy analysis of all ions produced in the interaction of low-energy primary ions ($E_0 < 5$ keV) with surface atoms is needed in order to obtain more meaningful and accurate results of elemental analysis and retrieve data on the specific features of the indicated interaction. In other words, a setup combining LEIS and secondary-ion mass spectrometry (SIMS) [8] is required. While this idea is not up-to-date [9], it was commonly implemented with the use of standard magnetic secondary-ion mass spectrometers, such as Cameca IMS-3f (4f) (see, e.g., [10]), and LEIS was regarded only as an additional tool with limited capabilities. The energy analysis of sputtered and scattered ions was performed by ramping the sample potential, resulting in changes in the energy of primary ions and the angles of scattering and entry of ions into the energy analyzer. The authors of [11]

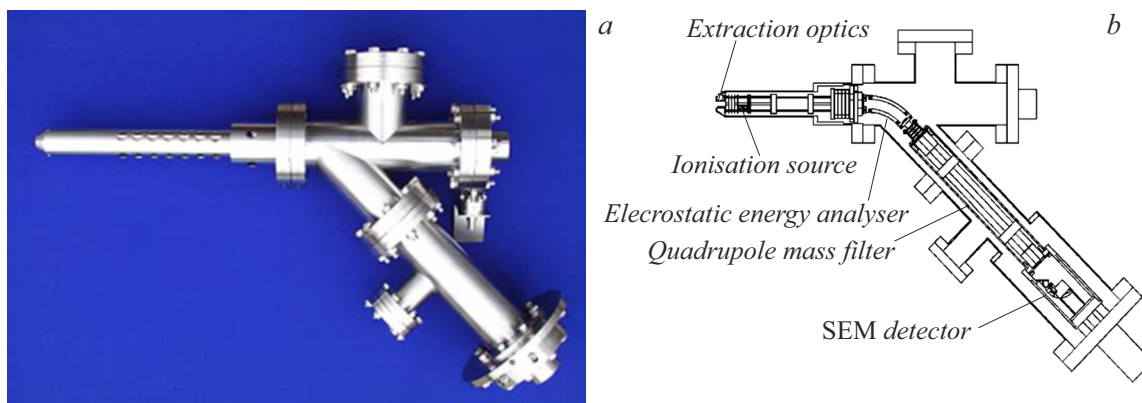


Figure 1. External view of an EQS 1000 mass-energy analyzer (a) and schematic diagram of its main functional parts (b).

used a DORAMIS quadrupole scanning ion microanalyzer fitted with a simple energy filter to carry out a joint mass and energy analysis of sputtered and scattered ions. This method was proposed to be called MARISS (mass-resolved ion scattering spectrometry). In the present study, we briefly discuss our approach to apparatus realization of MARISS along with the specifics of interpretation of experimental spectra acquired using this method (including those measured with argon primary ions).

An EQS 1000 mass-energy analyzer designed by Hiden (Warrington, Great Britain) is a key component of our experimental high-vacuum setup [12] assembled at Istituto per l'Energetica e le Interfasi (CNR-IENI, Padua, Italy). The external view of this instrument and its schematic diagram are shown in Figs.1, a and b, respectively. An extractor with an einzel lens and an ionizer with an electron source, which is designed for analysis of residual gases and ionization of neutral particles in the neutral-particle mass spectrometry mode, are located at the inlet. We had to redesign the extractor, since EQS was initially intended to be used for plasma analysis only, and the collection efficiency and transmission of the extractor decreased considerably in the MARISS mode with a fixed sample potential. The electric field and trajectories of sputtered and scattered ions were simulated using SIMION 3D within a wide energy range. Guided by the results of this simulation, we optimized the size and the shape of the extractor and the grounded shielding electrode.

The energy analysis was performed using a 45° cylindrical deflector with a system of quadrupole electrostatic lenses, and a quadrupole filter was used for mass spectrometry. An off-axis channel electron multiplier served as the ion detector. The energy analyzer was operated in the mode of constant transmission within the entire energy range of analyzed ions, and its energy resolution at passing energy $E_a = 80$ eV did not exceed $\Delta E_a = 3$ eV (FWHM). Ions separated in energy came to the quadrupole mass filter with a constant energy of 3 eV and a potential corresponding to E_a applied to its axis. The mass resolution of this filter remained unchanged at $\Delta M = 0.75$ amu (FWHM) throughout

the entire range of analyzed masses $M = 1-10^3$ amu. The EQS MASSoft software was used to control the operation of the mass and energy analyzer and process experimental data. An IQE 12/38 ion gun designed by SPECS (Berlin, Germany) served as the source of primary ions of inert gases (He^+ , Ne^+ , Ar^+).

Figure 2 shows the results of MARISS analysis of a jewellery alloy containing gold, silver, and copper. The examination of this alloy (produced by Top Finish in Florence, Italy) was performed under contract with an ordering party that obligated us not to disclose the quantitative composition gold assay of the alloy, since these data affect commercial interests of the company. The scale of energies of analyzed ions was converted using formula (1) into the scale of masses of surface atoms from which primary Ne^+ ions with energy $E_0 = 1$ keV were scattered by angle $\theta = 120^\circ$. The mass filter was adjusted so that ions of only the primary $^{20}\text{Ne}^+$ isotope would pass. It is noteworthy that the level of

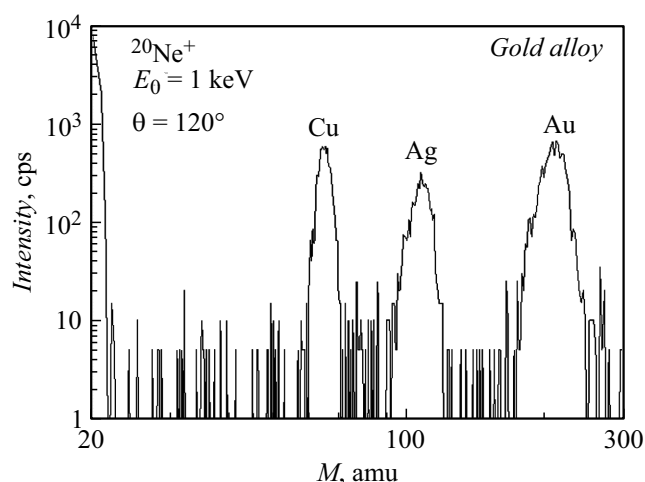


Figure 2. Mass-energy spectrum of Ne^+ ions with energy $E_0 = 1$ keV scattered by $\theta = 120^\circ$ from the surface of a jewellery alloy containing gold, silver, and copper. The scale of energies E of scattered ions was converted into the scale of masses M of surface atoms using formula (1).

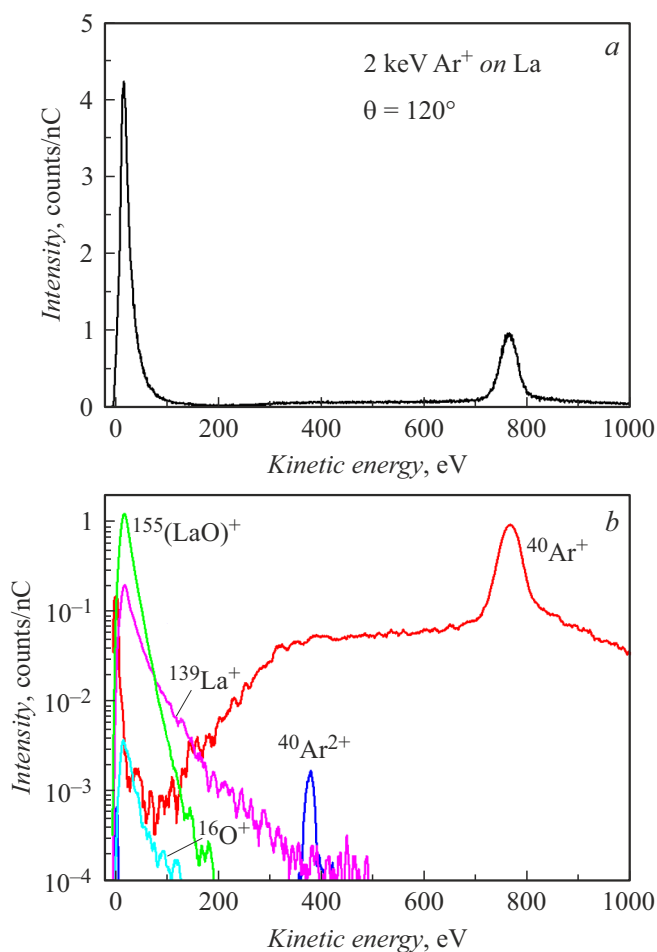


Figure 3. Energy distributions of sputtered and scattered ions measured under bombardment of a lanthanum sample by argon ions with an energy of 2 keV. *a* — energy analysis only, *b* — combined energy and mass-spectral analysis (MARISS spectrum).

noise was very low: it was attributable almost exclusively to intrinsic noise of the channel electron multiplier. This noise reduction contributes to an increase in MARISS sensitivity, since the sensitivity and, consequently, the detection limit of any analytical method depend on the ratio of intensities of the desired signal and noise. Thus, there is no need to approximate and subtract the noise component of a spectrum to determine the actual intensity of the signal of scattered ions in quantitative MARISS analysis. A detailed description of the specific features of quantitative MARISS analysis applied to a medieval Venetian denaro by Doge Enrico III and minted out of „billon“ (silver–copper alloy) was given in [13].

Figure 3 shows the spectra of scattering of argon ions with energy $E_0 = 2$ keV by angle $\theta = 120^\circ$ from the surface of a lanthanum sample. The spectrum in Fig. 3, *a* was measured in the energy analysis mode and is presented in a common form, while the spectrum in Fig. 3, *b* was obtained in the combined mass and energy analysis mode with a logarithmic intensity scale. Two peaks are apparent

in Fig. 3, *a*: a low-energy peak associated with sputtering of the sample surface by argon ions and a peak of elastic single Ar^+/La scattering. The data presented in Fig. 3, *b* are much more meaningful. The low-energy peak „decomposes“ into four peaks of sputtered atoms and molecules (specifically, atomic $^{139}\text{La}^+$ and $^{16}\text{O}^+$ ions, molecular $^{155}(\text{LaO})^+$ ions, and $^{40}\text{Ar}^+$ ions that were first implanted from the primary ion beam into lanthanum and then sputtered). Lanthanum is a chemically active element, and its untreated surface is always oxidized. The data in Fig. 3, *b* verify this assertion. The high-energy „tails“ of energy distributions of atomic lanthanum and oxygen ions are longer than those of molecular ions of lanthanum oxide. Intriguingly, the peak of sputtered $^{40}\text{Ar}^+$ ions in the spectrum is joined by a narrow and low-intensity peak with mass $M/Z = 20$, which belongs to doubly ionized sputtered $^{40}\text{Ar}^{2+}$ ions. As far as we know, this peak has not been observed earlier in spectra of sputtered ions. As for scattered ions, Fig. 3, *b* shows the $^{40}\text{Ar}^+/\text{La}$ spectrum with the peak of elastic single scattering from surface atoms and an intense background from argon ions that were scattered from lanthanum atoms in the near-surface sample volume and underwent inelastic energy losses. The peak of elastic scattering $^{40}\text{Ar}^{2+}/\text{La}$ of doubly ionized ions, which is „masked“ by the background of inelastically scattered $^{40}\text{Ar}^+/\text{La}$ ions, is also present. Note that a peak of doubly ionized argon ions scattered from a tungsten surface has been observed earlier in [14], although without a sputtered Ar^{2+} peak. Thus, the results of combined energy and mass-spectral analysis of scattered and sputtered ions were reported. This approach provides an opportunity to enhance the sensitivity of the ion scattering method by suppressing the sputtered-ion background and to obtain new experimental data regarding the surface state of chemically active lanthanum and the formation of doubly charged scattered and sputtered argon ions.

Funding

This study was supported in part under state assignment of the Ministry of Science and Higher Education of the Russian Federation (FSSN-2020-0003).

Conflict of interest

The authors declare that they have no conflict of interest.

References

- [1] E.S. Mashkova, V.A. Molchanov, *Primenenie rasseyaniya ionov dlya analiza tverdykh tel* (Energoatomizdat, M., 1995) (in Russian).
- [2] H.H. Brongersma, M. Draxler, M. de Ridder, P. Bauer, *Surf. Sci. Rep.*, **62** (3), 63 (2007). DOI: 10.1016/j.surfrep.2006.12.002
- [3] O. Grizzi, M. Shi, H. Bu, J.W. Rabalais, *Rev. Sci. Instrum.*, **61** (2), 740 (1990). DOI: 10.1063/1.1141488

- [4] H.H. Brongersma, T. Grehl, P.A. van Hal, N.C.W. Kuijpers, S.G.J. Mathijssen, E.R. Schofield, R.A.P. Smith, H.R.J. ter Veen, *Vacuum*, **84** (8), 1005 (2010). DOI: 10.1016/j.vacuum.2009.11.016
- [5] <https://www.iontof.com/qtac-low-energy-ion-scattering-leis-surface-analysis.html> (date of access 06.21.2022)
- [6] R.M. Singhanian, H. Price, V.Y. Kounga, B. Davis, P. Brüner, R. Thorpe, D.J. Hynek, J.J. Cha, N.C. Strandwitz, *J. Vac. Sci. Technol. A*, **39** (6), 063210 (2021). DOI: 10.1116/6.0001164
- [7] T.G. Avval, S. Pruša, S.C. Chapman, M.R. Linford, T. Šikola, H.H. Brongersma, *Surf. Sci. Spectra*, **28** (1), 014201 (2021). DOI: 10.1116/6.0000953
- [8] A. Benninghoven, F.G. Rüdener, H.W. Werner, *Secondary ion mass spectrometry. Basic concepts, instrumental aspects, applications, and trends* (Wiley, N.Y., 1987).
- [9] M. Grundner, W. Heiland, E. Taglauer, *Appl. Phys.*, **4** (3), 243 (1974). DOI: 10.1007/BF00884235
- [10] K. Franzreb, A. Pratt, S. Splinter, P. van der Heide, *Surf. Interface Anal.*, **26** (8), 597 (1998). DOI: 10.1002/(SICI)1096-9918(199807)26:8<597::AID-SIA399>3.0.CO;2-I
- [11] K. Wittmaack, *Surf. Sci.*, **345** (1-2), 110 (1996). DOI: 10.1016/0039-6028(95)00876-4
- [12] A. Tolstogousov, S. Daolio, C. Pagura, C.L. Greenwood, *Int. J. Mass Spectrom.*, **214** (3), 327 (2002). DOI: 10.1016/S1387-3806(02)00523-7
- [13] S. Daolio, C. Pagura, A. Tolstogousov, *Appl. Surf. Sci.*, **222** (1-4), 166 (2004). DOI: 10.1016/j.apsusc.2003.08.005
- [14] N.V. Mamedov, D.N. Sinelnikov, V.A. Kurnaev, D.V. Kolodko, I.A. Sorokin, *Vacuum*, **148**, 248 (2018). DOI: 10.1016/j.vacuum.2017.11.026